EEG Based User Recognition Using BUMP Modelling

Daria La Rocca*, Patrizio Campisi *, Jordi Solé-Casals **

*Section of Applied Electronics, Department of Engineering, University of Roma Tre,
Via Vito Volterra 62, 00146, Roma, Italy
daria.larocca@uniroma3.it, patrizio.campisi@uniroma3.it
** Escola Politècnica Superior, Universitat de Vic
C/ de la Laura, 13, 08500 Vic, Catalunya
jordi.sole@uvic.cat

Abstract: In this paper the use of electroencephalogram (EEG) as biometric identifier is investigated. The use of EEG within the biometric framework has already been introduced in the recent past although it has not been extensively analyzed. In this contribution we apply the "bump" modelling analysis for the feature extraction stage within an identification framework, in order to reduce the huge amount of data recorded through EEG. For the purpose of this study we rely on the "resting state with eyes closed" protocol. The employed database is composed of 36 healthy subjects whose EEG signals have been acquired in an ad hoc laboratory. Different electrodes configurations pertinent with the employed protocol have been considered. A classifier based on Mahalanobis distance have been tested for the enrollment of the subjects and their identification. An information fusion performed at the score level has shown to improve correct classification performance. The obtained results show that an identification accuracy of 99.69% can be achieved. It represents an high degree of accuracy, given the current state of research on EEG biometrics.

1 Introduction

EEG waves have been largely studied in the past with the aim of analyzing brain functioning, reflected in rhythmic activity of local or widespread neurons' networks during specific mental states. This activity can be measured extracting from the EEG signals the main brain rhythms involved in the integration of different processes, which show specific frequency content: $\delta([0.5-4]\text{Hz}), \theta([4-8]\text{Hz}), \alpha([8-14]\text{Hz}), \beta([14-30]\text{Hz})$ and $\gamma(\text{over } 30\text{Hz})$. The description of the brain functioning represented by EEG oscillations, recorded from the different scalp regions, is supposed to reflect individual-specific anatomical and psycho-physiological traits. In the last decade EEG signals have been proposed to be used in biometric based recognition systems. The aim of such frameworks is to detect and quantitatively evaluate inter-subject variability in EEG features, expected to show stability in an individual over time, as discussed in [CLRS12]. Some promising results have been obtained employing different EEG acquisition protocols, involving both resting conditions with closed or opened eyes, and response to specific internal or external events. EEG signals present some peculiarities, which are not shared by the most commonly used biometrics, like face, iris, and fingerprints. Specifically, brain signals, as a result of the electrical activity of the cortex, are not exposed like face, iris, and fingerprints. Therefore, they are more privacy compliant than other biometrics since they are "secret" by their nature, being impossible to capture them at a distance. This property makes EEG biometrics also robust against the spoofing attack at the sensor, since an attacker would not be able to collect and feed the EEG signals, which are the result of ionic current flows within the neurons of the brain. Moreover, being brain signals the result of a cognitive process, they cannot be synthetically generated and fed to a sensor, which also addresses the problem of liveness detection. Also, the level of universality of brain signals is very high. In fact people with some physical disabilities, preventing the use of biometrics like fingerprint or iris, would be able to get access to the required service using EEG biometrics. Due to a not practical acquisition process, also very sensitive to external and physiological noise, applications of EEG biometrics could be designed within high security contexts, given the actual technology. In fact, applications for everyday life access to personal utilities would result very impractical. Some interesting evidences have already been obtained in the recent literature, see for example [PRCE99], [BK10], [RSFC$^+$], [MdRM07], and [CSB$^+$11] where a review on the state of the art of EEG biometrics is also given. In the aforementioned papers, different acquisition protocols have been employed, such as closed or open eyes resting conditions, where the user is asked to rest and not to perform any specific task, or response to specific stimuli. Despite the promising results a systematic analysis of EEG biometric traits aiming at identifying individual specific features is missing.

The purpose of this work is to provide an analysis of parametric time-frequency maps of the acquired EEG signals, in order to identify distinctive measures of the map parameters for each individual. Therefore, in the proposed EEG-based biometric framework we focus on the features extraction stage, evaluating the significance of each considered variable in catching the differences between individuals. We rely on the resting state acquisition protocol to acquire data from 36 healthy subjects. Different configurations for the spatial placement of the electrodes are tested. Specifically, sets of three acquisition channels are considered selecting inter-hemispheric symmetrical configurations and combinations of mid-line electrodes. The analysis of each frequency band is also carried out in order to evaluate features of different brain rhythms, functionally involved in the integration of different kind of brain activities. The so acquired signals, after proper preprocessing, are then modeled employing wavelet decomposition to extract time-frequency maps. The wavelet analysis of EEG signals allows to obtain a dynamic representation of the frequency content able to catch even transient phenomena. The multi-scale approach allows to locate accurately time-frequency oscillations with different resolutions in the time-frequency space. Bump modelling of wavelet maps is subsequently performed in order to reduce the data dimensionality, and to provide relevant features. Fusion at the matching score level is also performed. The proposed system uses the combination of scores obtained considering different electrodes configurations and different frequency bands. A Mahalanobis distance based classifier is tested for identification purpose.

The paper is organized as follows. The employed modelling is detailed in Section 2, and in Section 3 the acquisition protocol, the template extraction stage and the classification procedure are described. Experimental results are given in Section 4, where the recognition performance is reported for all the tests carried out. Finally conclusions are drawn in Section 5.

2 Bump modelling

Given raw EEG signals collected thruogh a multi-channel EEG device, we seek to obtain a set of parameters allowing characterizing subjects from their brain electrical activity. In order to achieve this goal, we use bump modelling [VMD+07], which is a technique for modelling a timefrequency map, with the aim of representing the map with a limited number of elementary functions. The purpose is to reduce the huge quantity of parameters that describe a timefrequency map, tens to hundreds of thousands, to a sum of parametric functions, a few functions with some tens of parameters. These parameters will be used in order to characterize each subject.

The main idea of this method is to approximate a time-frequency map with a set of predefined elementary parameterized functions called bumps; therefore, the map is represented by the set of parameters of the bumps, which is a very sparse encoding of the map, resulting in information compression rates that range from one hundred to one thousand (rationales for this procedure, proofs and technical details are explained in [VMD+07]).

The algorithm performs the following steps on the time-frequency maps (after appropriate normalization):

i window the map in order to define the zones to be modelled (those windows form a set of overlapping sub-areas of the map);

ii find the window that contains the maximum amount of energy;

iii adapt a bump β to the selected zone, and withdraw it from the original map. The parameters of the bumps are computed using the BFGS algorithm [PFTV92] in order to minimize the cost function C defined by:

$$C = \frac{1}{2} \sum\nolimits_{t,f \in W} (z_{f,t} - \beta(f,t))^2 \tag{1}$$

where the summation runs on all pixels within the window W, $z_{f,t}$ are time-frequency coefficients at time t and frequency f, and $\beta(f,t)$ is the value of the bump function at time t and frequency f;

iv if the amount of information modelled by the bumps reaches a threshold, stop; else return to (iii).

EEG signals are transformed to time-frequency maps using Complex Morlet wavelets, as they are appropriate for time-frequency analysis of electroencephalographic signals because of its symmetrical and smooth Gaussian shape both in time and frequency domains [KMR87].

$$w(t) = \exp(-t^2/2{\sigma_t}^2)\exp(2i\pi r t) \tag{2}$$

Bump functions used are half ellipsoids. Half ellipsoids (see Figure 1) are defined by:

$$\begin{aligned} \beta(f,t) = a\sqrt{1-v} \quad & for \quad 0 \le v \le 1 \\ \beta(f,t) = 0 \quad & for \quad v > 1 \end{aligned} \tag{3}$$

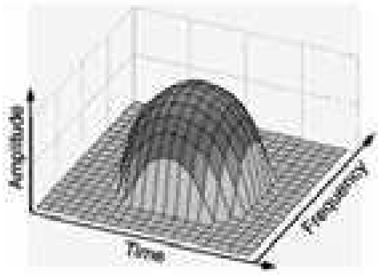

Figure 1: Half ellipsoid bump function.

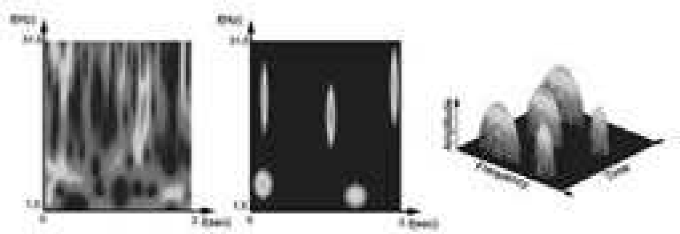

Figure 2: Left: normalized time-frequency map of an EEG recording; middle and right: 2D and 3D bump modeling of the map.

where $v = (e_f{}^2 + e_f{}^2)$ with $e_f = \frac{f-\mu_f}{l_f}$ and $e_t = \frac{t-\mu_t}{l_t}$. μ_f and μ_t are the coordinates of the center of the ellipsoid, l_f and l_t are the half-lengths of the principal axes, α is the amplitude of the function, t is the time and f the frequency.

Figure 2 shows a typical example of bump modelling of the time-frequency map of an EEG recording. Each bump is described by 5 parameters: its coordinates on the map (2 parameters), its amplitude (one parameter) and the lengths of its axes (2 parameters). All the experiments performed in this work have been done using the BUTIF Toolbox [VSCD$^+$09][1]

3 Data Analysis

In the data collection stage brain activity was recorded using a BrainAmp recording system, from Brain Products[2], operating at a sampling rate $S_r = 200Hz$. The EEG recordings of $N_C = 36$ healthy volunteers have been acquired. Informed consent was obtained from each subject after the explanation of the study, which was approved by the local institutional ethical committee. During the experiment, the participants were comfortably

[1] publicly available at: `http://www.bsp.brain.riken.jp/~fvialatte/bumptoolbox/toolbox_home.html`

[2] details on the amplifier device in `http://www.brainproducts.com/index.php`

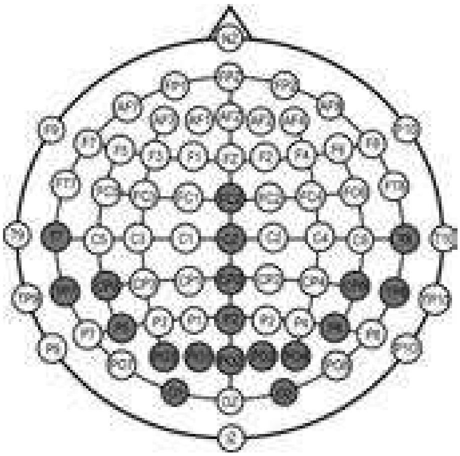

Figure 3: Electrodes positioning using the extended 10-20 international system.

seated in a reclining chair with both arms resting on a pillow in a dimly lit room, properly designed in order to minimize external sounds and noise, not interfering with the attention and the relaxed state of subjects. The EEG was continuously recorded from $C_T = 56$ sites on the scalp, positioned according to the $10 - 20$ international system as shown in Figure 3, and potentials were referenced to the average signal from the ear lobes. Before starting the recording session, the electrical impedance of each electrode was kept lower than 10kOhm through a dedicated gel maximizing the skin contact and allowing for a low-resistance recording through the skin. A set of $N_C = 36$ EEG digital recordings from $C_T = 56$ channels $V_i^{ch}[n]$, for $i = 1, \cdots, N_C$, $n = 1, \cdots, N_T$, and $ch = 1, \cdots, C_T$ has been obtained. The recorded signals have been consequently preprocessed as described in 3.2.

3.1 EEG acquisition protocol

Since the earliest applications of the EEG signals, particular interest has been shown in the study of cerebral activity during resting sate, due to the amount of information conveyed in it with respect to brain functioning and organization. Specific features of the brain activity during resting, as described by EEG signals, have given some indications about their capability to distinguish among people. In fact the resting state protocol has been employed in the biometric framework [ASLA10], [LRCS12] for recognition purpose. In the presented work we refer to EEG signals acquired during resting conditions. Specifically, the subjects were asked to perform one minute of “resting state with closed eyes”. Therefore in each session an $N_T = 200 \times 60$ samples long record was provided for each acquisition channel.

3.2 Preprocessing

In the preprocessing stage raw signals are first downsampled applying a decimation factor to the collected data. A sampling rate of $S_r = 100$Hz and its anti-aliasing FIR filter are selected according to the Nyquist theorem. A further band-pass filtering stage is applied after down-sampling in order to retain spectral information in the band $[0.5, 40]$Hz, containing most of the frequency components of interest referring to the resting state condition. The so obtained signals are then segmented into M overlapped frames of length T. A frame length of $T = 15s$ is selected, in order to achieve a trade-off between the sample size and the quality of the time-frequency decomposition at lower frequency range. Specifically, a time interval of one second is considered between the beginnings of consecutive frames. Such a considerable overlap resulting from the described segmentation is needed, due to the small sample size, in order to obtain an adequate number of instances which generate class distributions required when training the proposed classifier. $M = 45$ EEG overlapped frames are obtained for each subject and each channel. Subsequently the DC component is removed from each EEG segment, and a z-score normalization of each signal is performed in order to make signals referring to different acquisition sessions (users) reliably comparable, removing differences due to scale factors. The so obtained datasets, $\{Z_{i,m}^{ch}\}$, with $i = 1, \cdots, N_C$, $ch = 1, \cdots, C_T$, and $m = 1, \cdots, M$ is further processed to extract time-frequency maps from each user brain signal, as described in the following section.

3.3 Modelling and features extraction

In the herein proposed study, particular interest was directed to the data modelling in the time-frequency domain as described in Section 2. In more detail, for each subject i and each channel ch, the wavelet decomposition of EEG signals was computed employing Complex Morlet waveform, so that each frame m was represented by the extracted wavelet coefficients in the time-frequency space. The frequency range from 3Hz up to 40Hz was investigated, while lower frequencies were removed from the analysis, since the selected frame length limited the estimation accuracy of the related wavelet coefficients. Maps of coefficients were obtained analyzing the different brain rhythms θ, α, β and $\gamma[30-40]$Hz individually, as well as altogether. Therefore for each of the M EEG frames, five maps were provided $z_{f,t}^{b}$, with $b \in \{[3-40]\text{Hz}, \theta, \alpha, \beta, \gamma[30-40]\text{Hz}\}$. Bump modelling was then employed to obtain a parametric description of most energy contained in the wavelet maps, as described in Section 2. The publicly available BUTIF toolbox was used to extract the 5 parameters for each bump fitting the energy spots in the time-frequency representation of the EEG signals. Subsequently the analysis of the obtained parametric maps was performed in order to extract discriminant features, as reported in the following. A statistical analysis was carried out considering the median values for the amplitude (A), the central frequency (f_c), the volume (v), the surface of the meridian ellipse (a), the height (extension in frequency h) and the width (extension in time w) of the extracted bumps, modelling the time-frequency maps. Also we included in the analysis of features the total number of bumps for each map, the sum and max values of A, f_c, v, a, h and w, the number of bumps within different ranges of the investigated time-frequency domain, the amplitudes and central frequencies of bumps showing max values of parameters a, v, w

and h. Moreover for each bump map we obtained the spectral centroid $c(t)$, that is the "center of mas" of the bumps in the frequency domain defined for each time step t, computed as the weighted mean of the frequencies present in the map for each instant, with the corresponding map amplitudes as the weights. The average value over time of $c(t)$ was considered as a further feature. Furthermore, each of the listed parameters were also computed for filtered maps where a threshold value $\tau = 0.4$ was applied to the bump amplitude A. Therefore a feature vector of 39 components $\zeta_{tot} = [\zeta, \zeta_\tau]$ was obtained for each EEG frame, where parameters referred respectively to the unfiltered and the filtered maps were concatenated. The one-way Analysis of Variance (ANOVA) [Sch99] was performed in order to explore the within-subject and between-subjects variance of each feature extracted from the parametric time-frequency maps. Within the assumptions of normal distributions of features, homogeneity of variance of the different group distributions, and independence of observations, the null hypothesis to test was that data extracted from all groups (corresponding to subjects) show the same stochastic distribution, and that observed differences of values assumed by a certain feature between subjects is due to the case. According to the outcome of the test, the features which showed to vary significantly between subjects were selected to train the classifier for the recognition purpose. The so selected features were further tested performing the same ANOVA analysis for each pair of subjects, in order to verify the disjunction of all subjects from each-others. A final combination of features was selected, such that all pairs of subjects showed significant difference for most of them (at least two thirds). As a result of the statistical analysis, two thirds of the computed features were discarded and the remaining 13 discriminant parameters were considered to form the feature vector used to train and test the classifier. The features which individually showed to significantly discriminate group (subject) distributions with a confidence level of 99% are: the median value of A for both the unfiltered and filtered maps, the median value of v, the number of bumps within different adjacent ranges of the investigated time-frequency domain (6 elements), the number of bumps with $A > \tau$, the sum of the values of A for both the unfiltered and filtered maps, and the mean of $c(t)$ over time. Different spatial distributions of sets of three electrodes were considered, placed according to both symmetrical inter-hemispheric and mid-line configurations, as shown in Figure 3 with the marked electrodes. Features related to channels of each set under analysis were concatenated in a unique vector. Therefore, the resulting feature vector was obtained for each subject i, each set of channels Ch, each rhythm b and each frame m, providing a dataset ${}_{b}^{Ch}\hat{\zeta}_i(m)$ to evaluate the recognition performance as discussed below.

3.4 Classification

A linear discriminant analysis was performed for the identification purpose, in order to predict the class, namely the user identity, to which the observed feature vector $\hat{\zeta}$ belongs to. The model used for the discriminant analysis assumes that the vector $\hat{\zeta}$ has a Gaussian mixture distribution, the same covariance matrix for each class, and that only the means vary. The extracted feature vectors were divided into a training dataset $\hat{\zeta}^{train}$ used to enroll users, and a test dataset $\hat{\zeta}^{test}$ used to test the classification performance in terms of correct recognition. The correct recognition rate (CRR) we computed to evaluate the system's accuracy is defined as the average over the diagonal of the resulting misclassification matrix. It represents the percentage of test trials which led to a correct identification of each user within the cross-validation framework provided, averaged over the subjects. The classifier we implemented is based on the assumption of Gaussian mixture distribution drawn by the feature vectors of the training dataset. Mahalanobis distances, in squared units, are computed between each observation in the test dataset, that is feature vectors averaged over frames, and the mean of each of the N_C class distributions representing the training dataset. For each tested condition, the classification of the extracted feature vectors was carried out within a cross-validation framework providing 45 runs. In each cross-validation run a different partition of the entire dataset into training and test subsequent frames was provided, consecutively selecting one of the $M = 45$ frames to start the training. Due to the small sample dimension when considering 60 seconds EEG recordings, initial tests were carried out including overlapping frames between the train and test datasets in the analysis. In this initial experiments 35 frames were used to train the classifier and the remaining 10 frames to test the recognition accuracy. The best performing conditions were further examined removing the overlap between the training and test datasets, and the resulting performance shift was evaluated. In this latter case 20 consecutive frames were employed in the training stage, while only 5 consecutive frames form the test dataset. For each considered frequency band and each set of channels, the training stage consists of the evaluation of the class distributions of the feature vectors $\hat{\zeta}$, which were supposed belonging to the Gaussian mixture. In the test stage for each user j to be identified, the Mahalanobis distances $d(j,i)$ between the mean of the feature vectors $\hat{\zeta}_j^{test}$ and the means of the observed N_C class distributions μ_i were evaluated. For each considered vector a transformation of the classifier score $d(j,i)$ was obtained performing the multiplicative inverse $s(i,j) = 1/d(j,i)$. An information fusion integrating multiple sensors distributions and brain rhythms was then performed at the match score level, which is the most common approach in multibiometric systems [RNJ06]. The aim was to determine the best sets of channels configurations and frequency bands that could optimally combine the decisions rendered individually by each of them. The score fusion was obtained through the sum $\sum_b^{N_B} \sum_{Ch}^{S} s_{Ch}^b(i,j)$ of scores related to specific bands $b \in N_B$ and selected sets $Ch \in S$ composed of three electrodes. All tests performed and obtained results are reported in the next Section.

4 Results and Discussion

For the purpose of user identification EEG signals have been acquired from 36 subjects in resting conditions[3], and modelled in the time-frequency domain, in order to extract discriminant features. Bump modelling has been employed to reduce the dimensionality of the time-frequency representation of each EEG segment, while retaining most of the energy content, as discussed in Section 2. Within the feature extraction stage of the proposed biometric framework an extensive analysis of the parameters which describe the bump maps led to obtain a set of discriminant traits. Different tests have been carried out in order to infer about the best performant electrodes configuration and to analyze the distinctive contribution of each brain rhythm. More in detail, given the "resting state with eyes closed" acquisition protocol here investigated and the 56 employed channels shown in Figure 3, we considered different subsets of acquisition channels in order to find

[3]The authors thank prof. F. Babiloni Fondazione Santa Lucia, Rome, for having provided the dataset

the best performing spatial arrangements of the electrodes while minimizing their number. To achieve this goal we selected sets of three symmetrical inter-hemispheric and sets of mid-line electrodes. Template extraction has been performed as described in Section 3.3, by first preprocessing the EEG signals, which includes decimation with sampling rate $S_r = 100$Hz, band-pass filtering to remove very low and high frequency noise, z-score normalization and segmentation into overlapping frames of $T = 15s$. Then the so obtained frames are modeled through wavelet decomposition and parametric functions are used to obtain compact representations of the extracted wavelet coefficients in the time-frequency domain, employing the BUTIF toolbox. Different features have been extracted from the bump maps, and the analysis of variance was employed to evaluate the inter-subject variability of each of them, so that 13 features have been selected as discussed in Section 3.3. The subbands related to the different brain rhythms $\theta, \alpha, \beta, \gamma([30 - 40]\text{Hz})$, which are the ones interested by the "resting state with eyes closed" protocol, and their combination $[3 - 40]$Hz are individually modelled and analyzed. For each identity the template is subsequently obtained by concatenating the selected features related to the different electrodes in the set under analysis, thus generating feature vectors of length 13×3 for the sets of three electrodes listed in Table 2, first column.

In Table 1 the results obtained from the analysis of different subbands using the classifier based on the Mahalanobis distance, described in Section 3.4, are given for some of the tested electrodes configurations. The correct recognition percentages reported in the table refers to overlapped training and test datasets, and are obtained within a cross-validation framework as described in Section 3.4. In Table 2 the same analysis for a larger set of scalp electrodes configurations is provided considering disjoint datasets, which are obtained by removing overlapping frames. It is worth pointing out that the classification performance varies considerably for the different scalp regions and rhythms under analysis. Moreover the performance significantly decreases for the disjoint datasets than for the overlapped frames. On the other hand, the match score fusion obtained as discussed in Section 3.4 has led to a dramatic increase in recognition accuracy, especially for the otherwise poorly performing case of disjoint training and test datasets, as observed in Figure 4. For the selection of the frequency bands to combine, the best performing set of three channels $PO_3 - PO_z - PO_4$ (see Table 2) was considered, and subsequent score fusions were performed. To this aim the brain rhythms were sorted in descending order of performance achieved individually, and sequentially combined within a forward-backward stepwise approach, retaining in the information fusion only those bands which improved the correct classification. Results reported in Figure 4 showed that a significant improvement was obtained combining β, α and θ rhythms. The same approach was considered to select the combination of electrodes configurations, while considering the best performing band fusion $\beta \cup \alpha \cup \theta$. For the case of disjoint training and test datasets a correct recognition percentage of 99.69% could be achieved when the sets of three inter-hemispheric and mid-line channels $PO_3 - PO_z - PO_4, O_1 - PO_z - O_2, CP_5 - CP_z - CP_6, TP_7 - CP_z - TP_8, PO_1 - PO_z - PO_2, PO_z - P_z - CP_z, T_7 - C_z - T_8, P_5 - P_z - P_6, CP_z - C_z - FC_z$, and the three rhythms θ, α, β containing most information were combined into the match score fusion. It should be noticed that the selected channels result located in the posterior region of the head, where the considered rhythms are mainly detected. Figure 4 reports the improvements obtained in the subsequent steps of the information fusion. Moreover the re-

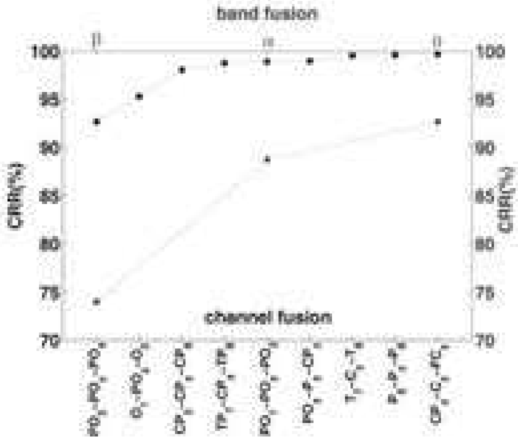

Figure 4: Improvement of the correct recognition rate obtained performing subsequent score fusions (see Section 4). Curves refer to the combination of different brain rhythms (top x-axis) and different electrodes sets (bottom x-axis). Labels in the x-axes refers to the score added at the related step.

sulting misclassification matrix showed that a 100% of correct identification was obtained for all users but one, who presented correct recognition rate of about 89%. The result obtained did not differ significantly from the perfect recognition performance (100%) obtained for the case of overlapped datasets, within the same information fusion approach and cross-validation framework.

5 Conclusions

In this paper the feature extraction from parametric representations of EEG signals, within the framework of EEG based biometric recognition, has been addressed. The simple "resting state with eyes closed" protocol has been employed to acquire a database of 36 people. Electrodes configurations have been selected in order to find the brain region containing the most significant information for the user identification purpose. Extensive simulations have been performed by considering different sets of 3 electrodes with respect to their positioning. Bump modelling has been employed for the parametric representation of the time-frequency maps, and the extraction of different features. Different subbands have been tested. In summary our analysis has shown that a very high degree of correct recognition can be achieved with a multibiometric approach consisting in an information fusion at the match score level, combining specific sets of electrodes configurations and brain rhythms.

A small set of features of parametric time-frequency maps obtained from EEG segments showed a significant variability between users, as observed from recognition accuracy obtained employing a simple Mahalanobis based classifier. In future works other classifiers could be considered in order to overcome the assumptions of the linear discriminant analysis, and to best fit the separation surfaces between the decision regions in the classification problem, since such surfaces are generally not hyper-planes. Different task performances

Channels	$3-40$Hz	θ	α	β	γ
C1 Cz C2	62.22	76.60	83.02	83.21	73.27
C3 Cz C4	73.27	84.26	87.10	87.90	76.67
C5 Cz C6	75.56	86.54	89.94	91.67	83.64
T7 Cz T8	78.83	85.43	93.09	92.96	85.19
PO1 POz PO2	79.69	86.23	90.43	93.77	79.01
TP7 CPz TP8	80.68	87.90	92.65	93.70	83.09
P7 Pz P8	81.60	89.44	94.57	92.90	83.33
O1 POz O2	82.59	86.30	94.14	94.38	83.70
PO3 POz PO4	84.69	**89.69**	**95.74**	**95.19**	83.21

Table 1: Classification performance in terms of correct recognition rate. Results refer to overlapped training and test datasets. The analysis of individual subbands is reposted in subsequent columns, and the set of 3 channels considered is listed in the first column.

Channels	$3-40$Hz	θ	α	β	γ
C1 Cz C2	24.81	38.61	43.70	45.65	35.56
CP1 CPz CP2	28.98	42.69	44.35	48.61	33.89
FCz Fz AFz	29.54	42.13	47.96	46.57	34.44
F3 Fz F4	29.63	41.02	54.35	51.39	38.98
Cz FCz Fz	30.19	39.17	49.07	46.85	39.44
CPz Cz FCz	30.46	44.81	49.72	53.70	41.02
C3 Cz C4	31.76	43.80	48.43	52.22	40.00
Pz CPz Cz	32.59	42.96	57.78	55.83	39.72
Fz AFz Fpz	34.17	38.43	44.63	51.20	31.30
CP5 CPz CP6	37.04	50.28	53.61	53.43	36.20
CP3 CPz CP4	37.59	45.09	49.35	55.28	36.76
FC3 FCz FC4	37.87	43.06	52.69	56.67	47.31
C5 Cz C6	40.00	46.11	57.78	58.70	48.98
P5 Pz P6	41.57	49.63	69.17	63.06	40.65
T7 Cz T8	42.41	42.41	62.41	62.69	50.09
POz Pz CPz	42.87	49.17	59.54	61.02	37.41
PO1 POz PO2	46.57	52.78	62.13	66.39	45.56
P7 Pz P8	46.94	53.98	71.11	62.31	47.50
TP7 CPz TP8	49.07	48.61	64.44	69.26	48.52
P3 Pz P4	49.91	45.28	64.91	62.04	43.98
O1 POz O2	52.59	51.57	64.91	69.91	52.04
PO3 POz PO4	52.78	**55.56**	**67.31**	**73.98**	49.81

Table 2: Classification performance in terms of correct recognition rate. Results refer to disjoint training and test datasets. The analysis of individual subbands is reposted in subsequent columns, and the set of 3 channels considered is listed in the first column.

could be also proposed for the acquisition of EEG signals to be represented through the bump modelling approach, in order to investigate the significance of the information related to the event timing for user recognition.

References

[ASLA10] M.K. Abdullah, K.S. Subari, J.L.C. Loong, and N.N. Ahmad. Analysis of the EEG Signalfor a Practical Biometric System. In *World Academy of Science,Engineering and Technology*, volume 68, page 1123, 2010.

[BK10] K. Brigham and B.V.K. Vijaya Kumar. Subject Identification from Electroencephalogram (EEG) Signals During Imagined Speech. In *Proceedings of the IEEE Fourth Int. Conf. on Biometrics: Theory, Applications and Systems (BTAS'10)*, 2010.

[CLRS12] P. Campisi, D. La Rocca, and G. Scarano. EEG for Automatic Person Recognition. *Computer*, 45(7):87–89, 2012.

[CSB+11] P. Campisi, G. Scarano, F. Babiloni, F. De Vico Fallani, S. Colonnese, E. Maiorana, and Forastiere L. Brain waves based user recognition using the eyes closed resting conditions protocol. In *IEEE International Workshop on Information Forensics and Security (WIFS'11)*, November 2011.

[KMR87] Grossmann A. Kronland-Martinet R., Morlet J. The wavelet transform. In C.H. Chen, editor, *Proceedings of IEEE Workshop on Expert Systems and Pattern Analysis*, pages 97–126. World Scientific, 1987.

[LRCS12] D. La Rocca, Patrizio Campisi, and Gaetano Scarano. EEG biometrics for individual recognition in resting state with closed eyes. In *Proceedings of the International Conference of the Biometrics Special Interest Group (BIOSIG)*, pages 1–12, 2012.

[MdRM07] S. Marcel and J. del R. Millan. Person Authentication Using Brainwaves (EEG) and Maximum A Posteriori Model Adaptation. *IEEE Trans. PAMI*, 29(4):743–748, 2007.

[PFTV92] William H Press, Brian P Flannery, Saul A Teukolsky, and William T Vetterling. *Numerical Recipes in FORTRAN 77: Volume 1, Volume 1 of Fortran Numerical Recipes: The Art of Scientific Computing*, volume 1. Cambridge university press, 1992.

[PRCE99] M. Poulos, M. Rangoussi, V. Chrissikopoulos, and A. Evangelou. Person identification based on parametric processing of the EEG. In *The 6th IEEE International Conference on Electronics, Circuits and Systems, (ICECS'99)*, pages 283–286, 1999.

[RNJ06] Arun A Ross, Karthik Nandakumar, and Anil K Jain. *Handbook of multibiometrics*, volume 6. Springer Science+ Business Media, 2006.

[RSFC+] A. Riera, A. Soria-Frisch, M. Caparrini, C. Grau, and G. Ruffini. Unobtrusive biometric system based on electroencephalogram analysis. *EURASIP J. Adv. Signal Process.*

[Sch99] H. Scheffé. *The Analysis of Variance*. A Wiley publication in mathematical statistics. Wiley, 1999.

[VMD+07] François B Vialatte, Claire Martin, Rémi Dubois, Joëlle Haddad, Brigitte Quenet, Rémi Gervais, and Gérard Dreyfus. A machine learning approach to the analysis of time–frequency maps, and its application to neural dynamics. *Neural networks*, 20(2):194–209, 2007.

[VSCD+09] François Vialatte, Jordi Solé-Casals, Justin Dauwels, Monique Maurice, and Andrzej Cichocki. Bump time-frequency toolbox: a toolbox for time-frequency oscillatory bursts extraction in electrophysiological signals. *BMC neuroscience*, 10(1):46, 2009.